

RESEARCH ARTICLE

 OPEN ACCESS

Received: 03-01-2024

Accepted: 01-06-2024

Published: 13-07-2024

Citation: Ghaly ST, Abadir MF, Sorour MA, Barakat FI (2024) Flow Properties of Tannery Waste Liquor. Indian Journal of Science and Technology 17(27): 2820-2828. <https://doi.org/10.17485/IJST/v17i27.20>

* **Corresponding author.**

sarahtarek04@cu.edu.eg

Funding: None

Competing Interests: None

Copyright: © 2024 Ghaly et al. This is an open access article distributed under the terms of the [Creative Commons Attribution License](https://creativecommons.org/licenses/by/4.0/), which permits unrestricted use, distribution, and reproduction in any medium, provided the original author and source are credited.

Published By Indian Society for Education and Environment ([iSee](https://www.isee.org/))

ISSN

Print: 0974-6846

Electronic: 0974-5645

Flow Properties of Tannery Waste Liquor

Sarah Tarek Ghaly^{1*}, M F Abadir¹, M A Sorour², F I Barakat¹

¹ The Chemical Engineering Department, Faculty of Engineering, Cairo University, Giza, Egypt
² Food Technology Research Center, Egypt

Abstract

Objective: A water treatment facility is to be erected nearby the industrial tanning complex, recently established East of Cairo, Egypt. This paper represents a contribution to studying the flow characteristics of the produced tannery waste effluents. A dried sample of tannery waste was chemically analyzed by X-ray fluorescence and its particle size distribution was determined. Next, rheological measurements were carried out on the waste slurry produced at temperatures ranging from 10°C to 40°C and three different solid concentrations, by weight: 20%, 25%, and 30%. The results showed that all waste suspensions under all conditions of solid content and temperature behaved as shear-thinning liquids. Flow indices of all suspensions generally tended to increase with temperature and solid concentration. Activation energies for viscosity were correlated to an increase in solid concentration and showed a decreasing pattern. All samples exhibited a thixotropic character that decreased with increased temperature and dilution of the suspension. The maximum pressure drops per unit length of a pipeline used to transport the waste suspension to the treatment unit was evaluated and found to increase with solid concentration and decrease with increasing temperature.

Keywords: Rheology; Tannery waste slurry; Solid content; Temperature

1 Introduction

Tannery waste represents a major nuisance as a water pollutant because of the presence of sulfides and chromium salts. According to the recent work of Appiah-Brempong et al. ⁽¹⁾, COD and BOD values of that waste can exceed 24300 mg.L⁻¹ and 2800 mg.L⁻¹ respectively. The treatment and management of tannery waste is an intricate process, the details of which were recently outlined by Zhao et al. ⁽²⁾, Sunmathi et al. ⁽³⁾, and Das et al. ⁽⁴⁾, who presented a comprehensive update on the status of the management of tannery waste in India, based on field studies involving 1600 tanneries. The pretreatment process involves a preliminary physical homogenizing step by agitating the suspension in a large tank. During this process, large coarse solids are separated. The next processing steps include the oxidation of sulfides and coagulation or flotation to remove fine solids.

Several attempts were made to make use of that waste. Riguette et al.⁽⁵⁾ have proposed the use of that waste in the preparation of adsorbent material, biodiesel, biogas, and biopolymers. Other uses were suggested by Tapia et al.⁽⁶⁾, as a source of animal fodder and by Amin et al.⁽⁷⁾ in the preparation of roof tiles.

In Egypt, a new tanning complex has been erected in a Cairo suburb (Egypt) that suffers from the disposal of the effluent waste streams emanating from more than two hundred tanneries agglomerated in that industrial area. Currently, it has been decided to erect a central wastewater treatment to recirculate waste to the industrial area. The presence of a water treatment facility therefore seems to be an absolute priority for an industrial tanning complex.

This has necessitated investigating the flow properties of tannery waste effluents to assist in designing the necessary equipment for that aim. In general, the flow properties of suspensions have been investigated by many researchers. Most suspensions have proved to exhibit non-Newtonian behavior⁽⁸⁾. The rheology of suspensions has proved to be mainly affected by the following factors: Solid concentration, temperature, and particle size distribution. The literature concerning the effect of solid concentration on rheological behavior traces well back to the forties of the last century and even earlier⁽⁹⁾. In all reported findings, there was a distinctive increase in apparent viscosity following an increase in the solids concentration of slurries⁽¹⁰⁾. According to most authors, shear thinning seems to be the most common type of non-Newtonian behavior followed by suspensions⁽¹¹⁾⁽¹²⁾, where the relation between shear stress τ and shear rate $\dot{\gamma}$ takes the form:

$$\tau = k \cdot \dot{\gamma}^n \quad (n < 1 \text{ and } k = \text{constant}) \quad (1)$$

The effect of temperature on the apparent viscosity of suspensions follows the well-known Arrhenius equation⁽¹³⁾:

$$\mu = A e^{\frac{E}{RT}} \quad (2)$$

This equation reveals an exponential decrease of viscosity with temperature (K). The parameter E in that equation is the activation energy ($\text{J} \cdot \text{mol}^{-1}$) whereas R is the general gas constant and A , a pre-exponential factor. The activation energy denotes the sensitivity of viscosity changes to a rise in temperature. This conclusion stems directly from Equation (2), which can be differentiated to give:

$$\left| \frac{d \ln \mu}{dT} \right| = \frac{E}{RT^2} \quad (3)$$

This shows that a decrease in E will cause a proportional decrease in the LHS, which represents the rate of variation of the logarithm of viscosity with respect to temperature.

Also, the effect of particle size and its distribution on the rheological properties of suspensions has been investigated by many authors. An increase in particle size was found to increase apparent viscosity and to decrease the flow index n in most shear thinning suspensions⁽¹⁴⁾⁽¹⁵⁾. On the other hand, Luckham et al.⁽¹⁶⁾ observed that broader particle size distributions corresponded to lower apparent viscosities.

On the other hand, the effect of solid concentration in suspensions on the viscosity was widely researched and a comprehensive review of the matter was detailed by Zhou et al.⁽¹⁷⁾. They suggested that for concentrated suspensions, the equation developed by Roscoe yielded results with reasonable accuracy:

$$\frac{\mu}{\mu_0} = \left(1 - \frac{\varphi}{\varphi_m} \right)^{-2.5} \quad (4)$$

In that equation, μ_0 represents the viscosity of pure fluid, φ is the volume fraction of solids and φ_m a constant depending on the particle size distribution and their geometry.

To the authors' knowledge, regarding the effect of different parameters on the rheology of tannery waste suspensions, scarce literature is available on the subject, none of which treated in detail these effects. In this respect, Ganesan et al.⁽¹⁸⁾ studied the effect of solid concentration on apparent viscosities of tannery sludge and found that the dynamic viscosity of samples aerated for different time periods increased with solid content. Also, Zhai et al.⁽¹⁹⁾ researched the effect of tannery sludge treatment on the rheology of the waste slurry and assumed a Hershel — Bulkley behavior during all stages of treatment. On the other hand, Cruz et al.⁽²⁰⁾ investigated the rheological behavior of mineral sludges, including the effect of the non-Newtonian behavior of these sludges on the different unit operations carried out during ore dressing. However, none of these works incorporated the effect of solid concentration or temperature on the rheological behavior of the sludge, nor did they consider the possibility of any thixotropic behavior.

In the present work, the rheology of samples of tannery waste sludge with different solid concentrations was investigated at temperatures ranging from 10 to 40°C, to simulate weather conditions encountered in Cairo. In this respect, the present work seems to be a first in that context, particularly since the scarce literature concerning the flow properties of tannery waste did not allude to any time-dependent behavior. Also, the prediction of the magnitude of the pressure drop associated with such suspensions has not been tackled in any previous study on tannery effluents. The present results can be used to predict the power required for transportation, pumping, and agitation of the slurry during the preliminary stage of physical treatment.

2 Methodology

2.1 Raw materials

The raw material used in this work is the same type previously used by one of the authors in a recent work concerning the reuse of that material⁽⁷⁾, namely tannery waste, kindly supplied from “Piel color” factory in Quesna, 50 km North of Cairo. Its chemical analysis is shown in Table 1 as determined by XRF analysis, AXIOS, PANalytical 2005, Wavelength Dispersive (WD-XRF) Sequential Spectrometer

The density of the waste was determined using the density flask method following ASTM D854 (2014). It was found to equal 0.8 g.cm⁻³.

Table 1. Chemical Analysis of tannery waste

Constituent	SiO ₂	Al ₂ O ₃	Fe ₂ O ₃	TiO ₂	CaO	MgO	Na ₂ O	K ₂ O	SO ₃	Cl ⁻	Total Cr oxides	LOI
Percent	3.54	0.63	0.74	0.02	4.12	11.54	4.18	0.04	7.6	3.37	23.24	39.6

The particle size distribution of the waste was determined in the present work and found to cover the size range of 0.044 – 4 mm. The median particle size $D_{50} = 0.13$ mm.

2.2 Experimental techniques

The rheology of the different aqueous suspensions of the waste was investigated using “Rheocalc (T2.1.52) rotational Brookfield viscometer”. This consists of a vertical spindle rotating in a small cup filled with slurry specimen. It is connected to a water bath for controlling the temperature. Each test needs a 15 ml. of sample. After the slurry was prepared, it was stirred for 2 min, before carrying out any measurements. As the spindle rotates in the liquid, the apparatus displays values of rotating speed (rpm), shear rate (s⁻¹), shear stress (Dyne.cm⁻²), and viscosity (cP). These values are displayed every 30 seconds. The tests were conducted on slurries with three solid concentrations (20, 25, and 30% by weight) and at four temperatures. Each test was repeated three times at each shear rate corresponding to a specific rpm, and an average value was taken. The range of shear rates used varied from 1 to 140 s⁻¹.

3 Results and Discussion

3.1 Introduction

According to field data, the solid concentration (by weight) in the effluent slurry varied from 20 to 30%. That is why, in the present work, three concentrations were chosen, namely, 20%, 25% and 30%.

3.2 Results with solid concentration 20%

When waste particles were suspended in water at 20% concentration, the flow behavior showed a shear thinning mode, as evident from Figure 1(a). The values of the parameters n and k are reproduced in Table 2, where the flow index generally decreased from 0.4318 to 0.2495 with increasing temperature, with a similar decrease in the pre-power constant k , in Equation (2). In Figure 2 (b), the corresponding curves for the variation of viscosity with shear rate exhibited a decrease towards an asymptotic zero value at the infinite shear rate, typical of shear-thinning fluids.

3.3 Results with a solid concentration 25%

The results obtained for the shear stress — shear rate curves of these samples also followed a shear thinning behavior in Figure 2 (a); although there was no clear trend for the variation of the flow index n with temperature, the value of that parameter varied

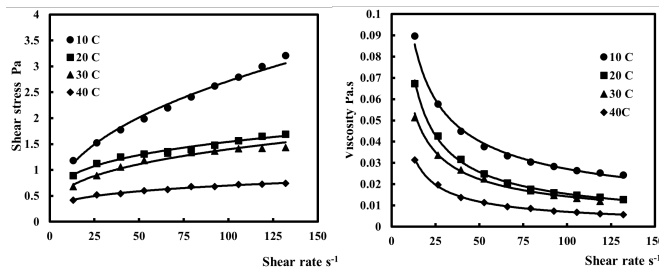


Fig 1. Rheological curves at 20% solid content

from 0.3276 to 0.4859 (Table 2). Also, the values of the parameter k generally decreased with increasing temperature. Figure 2 (b) illustrates the shear thinning tendency of viscosity — shear rate curves which are asymptotic to zero viscosity at infinite shear rate. Although the experimental points plotted at temperatures for the same shear rates 30 and 40°C are different, their fitted power functions remarkably coincided. (Figure 3).

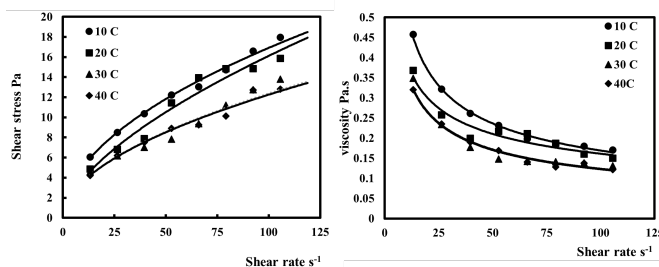


Fig 2. Rheological curves at 25% solid content

An interesting result that can be noticed by comparing Figure 2(a) and Figure 3 is the great rise in shear stress accompanying the increase in solid concentration from 20% to 25% at all temperatures investigated.

3.4 Results with a solid concentration of 30%

Upon increasing the solid concentration to 30%, the nature of flow remained shear thinning as can However, the values of shear stress recorded for the same shear rates at different temperatures were close, as evidenced by a crowding of stress – shear rates curves (not shown in figures). The decrease of viscosity with shear rate also revealed very close values of viscosities at the same shear rate. As for the flow index, there is a decreasing trend with increased temperature (Table 2) while its values generally increase with increasing solid content.

Table 2 summarizes the values obtained for the flow index n and pre-power factor k for the three solid contents investigated.

Table 2. Values of parameters n and k in Equation (1)

Temperature	10°C		20°C		30°C		40°C	
Parameters	n	k	n	k	n	k	n	k
20% solids	0.4318	0.3716	0.2615	0.4625	0.3124	0.3024	0.2495	0.2216
R ²	0.990		0.980		0.952		0.988	
25% solids	0.3276	3.359	0.4859	0.788	0.4065	0.857	0.4117	0.659
R ²	0.936		0.995		0.943		0.987	
30% solids	0.555	1.6628	0.5837	0.9496	0.5346	1.1414	0.4848	1.4245
R ²	0.988		0.987		0.985		0.957	

The values of viscosity determined for suspensions with different solid concentrations show a drastic increase as the concentration increased from 20% to 25%, while suspensions of 30% concentration showed a slight increase over those with 25% concentration. A similar effect was noticed by Ji et al. (21) in studying clay suspensions.

3.5 Variation of viscosity with temperature and solid content

The Arrhenius plots drawn for suspensions revealed a drop in activation energy following an increase in solid content. Figure 3 shows the results obtained for suspensions containing 20% solids at different shear rates. The values of activation energies calculated from the slopes of the straight showed generally a slight decrease in values on increasing shear rate.

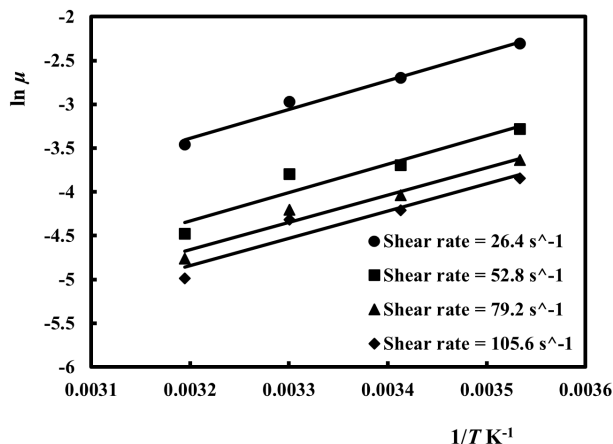


Fig 3. Arrhenius plots at different shear rates at 20% solid concentration

Table 3. Activation energy of viscosity at different solid concentrations (kJ.mol⁻¹)

Solid % (by weight)	20	25	30
$\dot{\gamma} = 26.4 \text{ s}^{-1}$	27.42	14.00	3.14
$\dot{\gamma} = 52.8 \text{ s}^{-1}$	27.03	12.46	3.07
$\dot{\gamma} = 79.2 \text{ s}^{-1}$	26.06	8.19	3.04
$\dot{\gamma} = 105.6 \text{ s}^{-1}$	25.93	8.21	3.05

A conclusion can be drawn from Table 3, that is, a regular decrease occurred in the values of activation energy of viscosity with increased solid content (Table 3). This means that the sensitivity of variations in viscosity with temperature highly decreases with increased solid content, as revealed by the extremely low values of activation energy determined at 30% solid.

3.6 Thixotropic behavior of waste suspensions

Although most studies involving thixotropy rely on using the area of the hysteresis loop formed by the up and down shear stress — shear rate curves⁽²²⁾, an alternative method was used in the present work, namely the exponential stretching theory⁽²³⁾. Following that theory, a parameter λ , indicating the extent of stability of the fluid-structure, is defined as follows:

$$\lambda = \frac{\mu(t) - \mu_{\infty}}{\mu_0 - \mu_{\infty}} \tag{5}$$

Here, μ_0 represents the viscosity at time = 0 (At a fixed value of shear rate), μ_{∞} is the final viscosity and $\mu(t)$, the viscosity at any intermediate time. This parameter is related to time by the following expression:

$$\lambda = e^{-\left(\frac{t}{\tau}\right)^n} \tag{6}$$

In this equation, τ represents the time constant. A low time constant corresponds to a limited thixotropic effect as the disturbed fluid structure will rearrange rapidly. This equation can be rearranged to read:

$$\ln(-\ln\lambda) = n\ln t - n\ln\tau \tag{7}$$

This way, a plot of $\ln(-\ln\lambda)$ against $\ln t$ should produce a straight line of slope n and intercept $n\ln\tau$, from which the value of the time constant τ can be deduced.

In the present work, it was first necessary to choose a suitable shear rate to be fixed to follow variations of viscosity values with time. This was chosen assuming a flow rate of $200 \text{ m}^3 \cdot \text{h}^{-1}$ and a pipe diameter of 6" (0.1524 m), as will be explained in the next section. This corresponds to an average velocity of $3.07 \text{ m} \cdot \text{s}^{-1}$. The corresponding shear rate can then be calculated from the following expression⁽²⁴⁾:

$$\dot{\gamma} = 8v/D = 161 \text{ s}^{-1}.$$

Therefore, tests were performed at the highest available shear rate of 132 s^{-1} , to approximate the practical situation.

To avoid any redundancy, only the results at a solid concentration of 20% are presented. For the two other solid concentrations, only the final results are reported.

Figure 4 shows the variation of viscosity with time at the fixed shear rate for different temperatures. The viscosity–time curves approach fixed values after about 5 minutes (300 s).

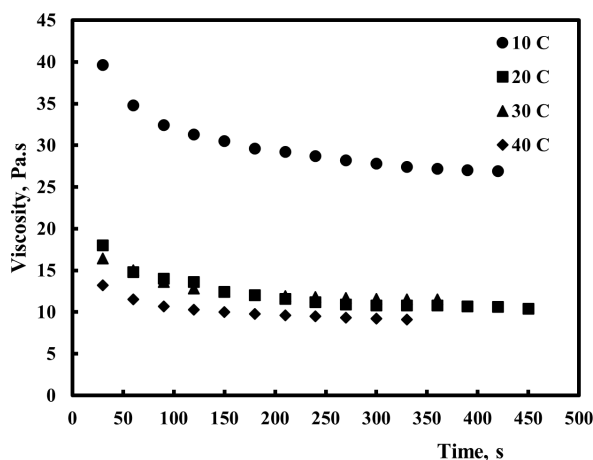


Fig 4. Variation of viscosity with time at shear rate = 132 s^{-1}

The plots of $\ln(-\ln\lambda)$ against $\ln t$ were carried out at the four temperatures investigated. Figure 5 illustrates the plot obtained at 10°C . The slopes and the intercepts of the lines were determined, and values of time constants were calculated. Table 4 summarizes the findings at the four temperatures.

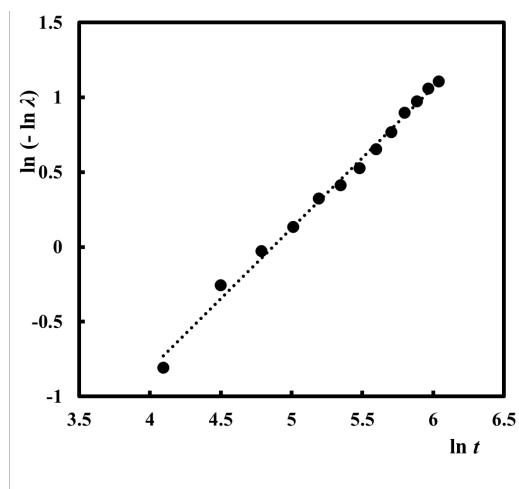


Fig 5. Plot of $\ln(-\ln\lambda)$ against $\ln t$ at 10°C

Table 4 indicates, among other parameters, that the extent of thixotropy, as revealed by the values of time constant, generally decreases with increased temperature and with dilution of the suspension. This result can be easily interpreted since the reconstruction of a new structure is faster at higher temperatures and at low solid concentrations.

3.7 Prediction of pressure drop in a draining line

To conclude, it was found interesting to make use of the experimental data in assessing the maximum pressure drop that can show in the pipeline that conveys the waste suspension to the treatment unit. The maximum pressure drop will be related to maximum viscosity, that is the viscosity recorded at 10°C.

Some basic assumptions have been made to that effect; data being obtained from the tannery from which the waste was retrieved:

1. In that plant, waste slurry is being collected in a tank and subsequently delivered to the treatment plant at a rate of 1.2 m³.h⁻¹. However, the government currently aims at erecting a treatment plant to deal with the totality of waste generated by more than 200 leather tanneries. Consequently, a central tank will be installed to collect streams from all tanning units. The waste suspension flow rate from that tank to the treatment plant will be assumed to be 200 m³.h⁻¹ (0.056 m³.s⁻¹)

2. The connecting pipeline is 6" in diameter (0.1524 m). Consequently, for the given flow rate, the velocity of flow can be determined. It was found to equal 3.07 m.s⁻¹.

The corresponding shear rate can then be calculated from the expression⁽²⁴⁾ : $\dot{\gamma} = 8v/D = 161 \text{ s}^{-1}$.

The following equation was used to predict the pressure drop per unit length of the pipe $\frac{\Delta p}{L}$ (Pa.m⁻¹) for shear thinning fluids⁽²⁵⁾:

$$Q = \pi \left[\frac{n}{3n+1} \cdot \left(\frac{\Delta p}{2k.L} \right)^{\frac{1}{n}} \right] r^{\frac{3n+1}{n}} \quad (8)$$

In that expression, the parameters k and n are defined by Equation (1) ; Q is the flow rate (m³.s⁻¹), L is the length of the pipe and r its internal radius (m).

From Table 2 :

$$n = 0.555, k = 1.6628$$

Substituting in Equation (7), one gets:

$$\Delta p/L \approx 811 \text{ Pa.m}^{-1}$$

For higher temperatures, the calculated values of $\Delta p/L$ were as follows:

$$\text{At } 20^\circ\text{C: } \Delta p/L = 532 \text{ Pa.m}^{-1}$$

$$\text{At } 30^\circ\text{C: } \Delta p/L = 504 \text{ Pa.m}^{-1}$$

$$\text{At } 40^\circ\text{C: } \Delta p/L = 492 \text{ Pa.m}^{-1}$$

The expected result that an increase in the temperature of suspensions results in lower pressure drops is an obvious result owing to decreased viscosity.

4 Conclusions

Rheological measurements were carried out for the tannery waste produced by a plant situated North of Cairo (Egypt) to elucidate the flow behavior of that sludge, as similar research work was found to be extremely scarce. The concentration of solids (By weight) in the waste stream was varied from 20 to 30% and temperatures from 10 to 40°C to simulate actual conditions found in practice. The following results were obtained:

Particle size analysis of the solid waste showed that about 75% of the particle sizes were situated between 0.075 and 0.300mm.

Waste suspensions, under all conditions of solid content and temperature behaved as shear thinning liquids. The effect of the different parameters investigated on the shear stress can be summarized by the 3D representation shown in Figure 6. This was drawn at the highest available shear rate in the experimental setup (132 s⁻¹), to simulate as much as possible the conditions at the calculated value of 161 s⁻¹ (for the assumed industrial setup). It reveals a decrease of shear stress with increased temperature and decreased solid concentration.

Viscosities of all suspensions investigated tended to decrease with temperature and increase with solid content. The activation energy of viscosity, denoting the sensitivity of viscosity with respect to temperature showed a decrease in value with increased shear rate and solid concentration. This implied that the sensitivity of variation of viscosity to changes in temperature decreased with increased solid concentration.

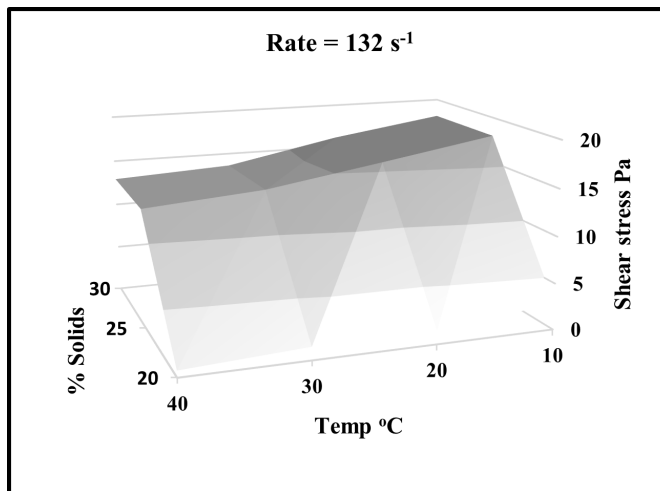


Fig 6. 3D Plots for the combined effect of different parameters on shear stress

The different sludge samples exhibited thixotropic behavior that decreased with increased temperature and with dilution of the suspension.

Preliminary calculations for pressure drop along the pipeline conveying the liquid waste to a treatment plant showed that the maximum pressure drop per unit length decreased with temperature and lower solid contents.

The comprehensive Table 4 provides a summary of the main findings of the work including the steady state viscosity (mPa.s) at a shear rate of 132 s⁻¹, a value in the range encountered in practice, the time constants (s) indicating the extent of thixotropy, and the pressure drop per unit length of pipe (Pa.m⁻¹) as a function of temperature and solid concentration. Besides, the activation energy for viscosity was shown as a function of solid concentration (kJ.mol⁻¹) at the previously indicated shear rate.

Table 4. Values of flow parameters of tannery sludge

Temp °C	20%			25%			30%		
	μ	τ	$\Delta p/L$	μ	τ	$\Delta p/L$	μ	τ	$\Delta p/L$
10	2.43	130.15	783	17.1	177.23	802	18.8	209.47	811
20	1.28	118.18	469	13.2	140.63	511	17.5	206.17	532
30	1.26	111.69	423	13.1	130.77	468	16.7	200.68	504
40	0.56	107.14	398	12.0	114.24	422	15.3	196.68	492
E		25.93			8.21			3.05	

From this table, the following conclusions can be drawn:

The effect of solid concentration on viscosity is lowest at higher concentrations, as revealed by the minor changes as the temperature is raised from 10 to 40 °C, and the low activation energy associated. It is also apparent that there is a minor increase only in pressure drop following increased concentration.

The thixotropic behavior of the suspension will cause a drop in viscosity when the slurry is agitated at constant speed in the preliminary homogenizing tank, since the viscosity will tend to drop at constant shear rate. The thixotropic effect of concentrated suspensions, as revealed by their higher time constant, increases with increased solid content.

This means that it is unnecessary to dilute the tannery waste slurry as it leaves the tannery, thus consuming less water in the process.

In suburban Cairo, where the tannery complex is located, the temperature rarely drops below 10 °C, even by night, while it usually exceeds 30 °C from April to November, by day. Consequently, the conveying pipes need not be insulated since a higher temperature will entail lower power consumption.

In future research regarding sludges in general, and tannery sludge in particular, more emphasis should be placed on the effect of particle size and particle size distribution on the suspended solids on the rheological behavior of the sludge.

References

- 1) Appiah-Brempong M, Essandoh H, Asiedu NY, Dadzie SK, Momade F. Artisanal tannery wastewater: quantity and characteristics. *Heliyon*. 2022;8(1). Available from: <https://doi.org/10.1016/j.heliyon.2021.e08680>.
- 2) Zhao J, et al. Tannery wastewater treatment: conventional and promising processes, an updated 20-year review. *J Leather Sci Eng*. 2022;4(1). Available from: <https://doi.org/10.1186/s42825-022-00082-7>.
- 3) Sunmathi N, Padmapriya R, Sudarsan JS, Nithiyantham S. Optimum utilization and resource recovery of tannery sludge: A review. *Int J Environ Sci Technol*. 2023;20(9):10405–10414. Available from: <https://doi.org/10.1007/s13762-022-04483-3>.
- 4) Das I, Srinivasan SV, Kumar A, Vidyarthi AK, Singh RK. Tannery Waste Management in India: A Case Study. In: D M, editor. Sustainable Advanced Technologies for Industrial Pollution Control. ATIPC 2022. Springer Proceedings in Earth and Environmental Sciences. Springer. 2022. Available from: https://doi.org/10.1007/978-3-031-37596-5_23.
- 5) Rigueto C, Rosseto M, Krein D, Ostwald B, Massuda LA, Zanella BB, et al. Alternative uses for tannery wastes: a review of environmental, sustainability, and science. *J Leather Sci Eng*. 2020;2(21). Available from: <https://doi.org/10.1186/s42825-020-00034-z>.
- 6) Tapia N, Moina HB. Exploring tannery solid wastes as a source of animal feed. *Processes*. 2023;11(10):2965–2965. Available from: <https://doi.org/10.3390/pr11102965>.
- 7) Shk A, Ashmawy N, Abadir MF. The use of tannery waste in the preparation of clay roof tiles. *Const Build Mater*. 2022;325:126393–126393. Available from: <https://doi.org/10.1016/j.conbuildmat.2022.126393>.
- 8) Tanner R. Review: Rheology of noncolloidal suspensions with non-Newtonian matrices. *J Rheol*. 2019;63:705–705. Available from: <https://doi.org/10.1122/1.5085363>.
- 9) Ghanaatpishehsanaei G, Rajinder P. Rheology of suspensions of solid particles in liquids thickened by starch nanoparticles. *Colloids Interface*. 2023;7(3):52–52. Available from: <https://doi.org/10.3390/colloids7030052>.
- 10) Ji X, Liang Y, Cao W. Effect of Solid Volume Concentration on Rheological Properties of Chengdu Clay Slurry. *Processes*. 2022;10(2):425–425. Available from: <https://doi.org/10.3390/pr10020425>.
- 11) Papadopoulou A, Gillissen JJ, Wilson HJ, Tiwari MK, Balabani S. On the shear thinning of non-Brownian suspensions. *J Non-Newtonian Fluid Mech*. 2020;28. Available from: <https://doi.org/10.1016/j.jnnfm.2020.104298>.
- 12) Trofa M, Avino D, G. Rheology of a dilute suspension of aggregates in shear-thinning fluids. *Micromachines*. 2020;11(4):443–451. Available from: <https://doi.org/10.3390/mi11040443>.
- 13) Burlawar S, Klingenberg DJ, Root TW, Scott CT, Houtman CJ, Bourne KJ. Effect of temperature on the rheology of concentrated suspensions containing lignocellulosic biomass particles. *Biomass Bioenergy*. 2022;156:106298–106298. Available from: <https://doi.org/10.1016/j.biombioe.2021.106298>.
- 14) Nguyen TC, Fillaudeau L, Anne-Archard, Chu-Ky D, Luong S, Vu HN, et al. Impact of particle size on the rheological properties and amylolysis kinetics of ungelatinized cassava flour suspensions. *Processes*. 2021;9(6):989–989. Available from: <https://doi.org/10.3390/pr9060989>.
- 15) Liu Y, Zhang Q, Liu R. Effect of particle size distribution and shear rate on relative viscosity of concentrated suspensions. *Rheologica Acta*. 2021;60:763–774. Available from: <https://doi.org/10.1007/s00397-021-01301-4>.
- 16) Luckham PF, Ukeje MA. Effect of particle size distribution on the rheology of dispersed systems. *J Colloid Interface Sci*. 1999;220(2):347–356. Available from: <https://doi.org/10.1006/jcis.1999.6515>.
- 17) Zhu Z, Wang H, Peng D. Dependence of sediment suspension viscosity on solid concentration: A simple general equation. *Water*. 2017;9(7):474–474. Available from: <https://doi.org/10.3390/w9070474>.
- 18) Ganesan V, Muthulakshmi B. Study on rheology and optimization for treating tannery effluents in submerged aerobic membrane bioreactor. *Int J Innov Eng Tech*. 2015;6(2):53–60. Available from: <https://rb.gy/lhsuvq>.
- 19) Zhai S, Xiong Y, Li M, Wang D, Fu S. Roles of hydrothermal-alkaline treatment in tannery sludge reduction: rheological properties and sludge reduction mechanism analysis. *RSC Adv*. 2020;10(24):14291–14298. Available from: <https://doi.org/10.1039/C9RA11010K>.
- 20) Cruz N, Forster J, Bobicki ER. Slurry rheology in mineral processing unit operations: A critical review. *Can J Chem Eng*. 2019;97:2102–2120. Available from: <https://doi.org/10.1002/cjce.23476>.
- 21) Ji X, Liang Y, Cao W. Effect of Solid Volume Concentration on Rheological Properties of Chengdu Clay Slurry. *Processes*. 2022;10(2):425–425. Available from: <https://dx.doi.org/10.3390/pr10020425>. doi:10.3390/pr10020425.
- 22) Cayeux E, Leulsegue A. The Effect of Thixotropy on Pressure Losses in a Pipe. *Energies*. 2020;13(23):6165–6165. Available from: <https://dx.doi.org/10.3390/en13236165>.
- 23) Wei Y, Solomon MJ, Larson RG. Quantitative nonlinear thixotropic model with stretched exponential response in transient shear flows. *Journal of Rheology*. 2016;60(6):1301–1315. Available from: <https://dx.doi.org/10.1122/1.4965228>.
- 24) Chabra RP, Richardson J. Non-Newtonian Flow in the Process Industries. *Butterworth - Heinemann Ed*. 1999;p. 74–76. Available from: <https://doi.org/10.1016/B978-0-7506-3770-1.X5000-3>.
- 25) Li Z, Zheng L, Huang W. Rheological analysis of Newtonian and non-Newtonian fluids using Marsh funnel: Experimental study and computational fluid dynamics modeling. *Energy Sci Eng*. 2020;8(6):2054–2072. Available from: <https://doi.org/10.1002/ese3.647>.